Quantitative in Situ Studies of Ionic Doping of Polypyrrole Employing Rotated Ring−Disk Electrode Voltammetry

Corey A. Salzer and C. Michael Elliott*

Department of Chemistry, Colorado State University, Fort Collins, Colorado 80523

Received January 10, 2000. Revised Manuscript Received March 1, 2000

Changes in ionic composition (i.e., doping) accompany changes in the redox level of conducting polymers such as polypyrrole. These processes are of paramount interest because they often control the polymer's charge capacity and, more importantly, its rates of oxidation and reduction (i.e., charge and discharge). The most commonly used approaches for studying polymer doping are either ex situ techniques (e.g., elemental analysis, X-ray photoelectron spectroscopy) or nonspecific techniques (e.g., electrochemical quartz crystal microgravimetry). We have developed a paradigm whereby rotated ring−disk electrode (RRDE) voltammetry can be used to quantitatively measure both anion and cation fluxes, in situ, across the conducting polymer−solution interface. This can be accomplished in real time under operational electrochemical conditions. Herein we report studies where we use RRDE voltammetry to investigate the doping behavior of electrochemically grown films of polypyrrole which are in contact with a range of different electrolyte solutions.

Introduction

During the electrochemical oxidation of pyrrole to form electrode-bound films of polypyrrole (pPY), anions are incorporated to maintain charge neutrality. To change the redox state of the polymer film, counterions (i.e., dopants) must exchange between the polymer and solution. In the specific case of polypyrrole, anion flux is expected to dominate doping changes provided the anions are readily mobile. If they are not, cation flux can become involved and can even become dominant. In other words, immobile anions within polypyrrole (or any analogous polymer) can be charge compensated during polymer reduction by cation uptake. In fact, as we will show subsequently, under the right conditions, fluxes of anions and cations can occur simultaneously at the polymer solution/interface during changes in the doping level.

Generally, the ion transport behavior of polymers can be affected by many parameters. For electrochemically deposited films of conventional organic conducting polymers (e.g., polypyrroles, polythiophenes, polyanilines, etc.), these include the identity of polymerizable monomer(s),[1,2] the counterion incorporated during film growth,[3−6] and the nature of the solvent and electrolyte utilized in subsequent electrochemistry.[3,5,7−10] Furthermore, the chemical and physical stability of a polymer, its rates of charge/discharge, and its total charge capacity during redox cycling are all also properties that are intimately related to the doping process. Given the considerable attention this class of materials has attracted, it should not be a surprise that there is a continuing interest in devising quantitative approaches to characterizing ion and solvent transport across polymer−solution interfaces under operational electrochemical conditions.

Several analytical methods have been employed in attempts to investigate ion transport associated with conducting polymers. These techniques include X-ray photoelectron spectroscopy,[3,11,12] fluorescence techniques,[13,14] scanning electrochemical microscopy,[15] and electrochemical quartz crystal microgravimetry (EQCM).[12,14,16−21] While each approach has its advantages, each has limitations in its ability to quantitatively and specifically monitor the ion flux for a wide range of

(1) Delabouglise, D. *Synth. Met.* **1992**, *51*, 321.
(2) Schiavon, G.; Zotti, G.; Comisso, N.; Berlin, A.; Pagani, G. *J. Phys. Chem.* **1994**, *98*, 4861.
(3) Ren, X.; Pickup, P. G. *J. Phys. Chem.* **1993**, *97*, 5356.
(4) Naoi, K.; Lien, M.; Smyrl, W. H. *J. Electrochem. Soc.* **1991**, *138*, 440.
(5) Zhou, Q.-X.; Kolaski, C. J.; Miller, L. L. *J. Electroanal. Chem.* **1987**, *223*, 283.
(6) Vorotynsev, M. A.; Vieil, E.; Heinze, J. *J. Electroanal. Chem.* **1998**, *450*, 121.
(7) Duffitt, G. L.; Pickup, P. G. *J. Phys. Chem.* **1991**, *95*, 9634.
(8) Mao, H.; Pickup, P. G. *J. Phys. Chem.* **1989**, *93*, 6480.
(9) Iseki, M.; Ikamatsu, M.; Sugiyama, Y.; Kuhara, K.; Mizukami, A. *J. Electroanal. Chem.* **1993**, *358*, 221.
(10) Elliott, C. M.; Kopelove, A. B.; Albery, W. J.; Chen, Z. *J. Phys. Chem.* **1991**, *95*, 1743.
(11) Bach, C. M. G.; Reynolds, J. R. *J. Phys. Chem.* **1994**, *98*, 13636.
(12) Bose, C. S. C.; Basak, S.; Rajeshwar, K. *J. Phys. Chem.* **1992**, *96*, 9899.
(13) Krishna, V.; Ho, Y.-H.; Rajeshwar, K. *J. Am. Chem. Soc.* **1991**, *113*, 3325.
(14) Reynolds, J. R.; Pyo, M.; Qiu, Y.-J. *Synth. Met.* **1993**, *55*, 1388.
(15) Arca, M.; Mirkin, M. V.; Bard, A. J. *J. Phys. Chem.* **1995**, *99*, 5040.
(16) Lien, M.; Smyrl, W. H.; Morita, M. *J. Electroanal. Chem.* **1991**, *309*, 333.
(17) Baker, C. K.; Qui, Y.-J.; Reynolds, J. R. *J. Phys. Chem.* **1991**, *95*, 4446.
(18) Lim, J. Y.; Paik, W.; Yeo, I.-H. *Synth. Met.* **1995**, *69*, 451.
(19) Li, Y.; Liu, Z. *Synth. Met.* **1998**, *94*, 131.
(20) Hillman, A. R.; Loveday, D. C.; Bruckenstein, S. *J. Electroanal. Chem.* **1989**, *274*, 157.
(21) Hillman, A. R.; Swann, M. J.; Bruckenstein, S. *J. Electroanal. Chem.* **1990**, *291*, 147.

10.1021/cm0000189 CCC: $19.00
Published on Web 07/08/2000

experimental conditions. For example, EQCM, which is the most commonly employed means of studying the doping process, monitors changes in polymer composition by measuring changes in film mass during electrochemical cycling. Although it is a sensitive in situ technique, it lacks the specificity to unambiguously distinguish between different ion types or between ions and solvent; thus, there is an inevitable ambiguity about compositional changes determined by EQCM. A case in point is the polymer formed by oxidizing pyrrole in a solution containing poly(styrenesulfonate) (pPY^+/pSS^-). Several studies of this composite material,[3,4,22,23] including one of our own,[10] had implicated cation transport in doping changes. All were inconclusive because no means was available to selectively and quantitatively monitor cation flux. In response to this need, we developed an approach based on rotated ring−disk electrode (RRDE) voltammetry which ultimately allowed us to directly follow the flux of cations across the pPY^+/pSS^-−solution interface in real time.[24] *We were able to show that, under fairly typical electrochemical conditions, doping changes in this composite involve exclusively cation transport.*

Doping level changes in conventional noncomposite organic conducting polymers (e.g., polypyrrole doped with small anions such as PF_6^-) can be considerably more complex than in pPY^+/pSS^- because, as we will demonstrate, it is possible for both cations and anions to be involved. Moreover, doping ion profiles typically depend on the identities of the ions available,[3,24] the potential applied to the polymer,[6] and its history. Consequently, doping studies involving these types of polymers present a much more formidable challenge. In principle, however, the same RRDE approach used successfully to quantitate doping changes in pPY^+/pSS^- can be adapted to study other polymers. What is required is the ability to independently monitor both cation and anion fluxes.

The details of how RRDE voltammetry can be applied to study ion flux across polymer−solution interfaces are given in ref 24; thus, they will not be duplicated here. Nevertheless, before embarking on a discussion of the results of the present study, it is useful to provide a brief synopsis of how this approach works. First, the ion to be monitored (probe ion) is chosen such that it has a mass-transport-limited redox process within the solvent window but is electrochemically inactive over the potential range of the polymer's electroactivity. Also, a supporting electrolyte is present in solution that, ideally, is totally excluded from the bulk of the polymer by virtue of its physical size. Typically, the electroactive probe ion is at a concentration an order of magnitude lower than that of the large electrolyte ions, thus minimizing migration effects. While the electrode is rotated, the potential of the ring is set to give mass-transport-limited oxidation or reduction of the probe ion. Ideally, in the absence of any polymer redox chemistry at the disk, a *time-independent* current passes at the ring, $i_{r,0}$. When the potential at the disk is scanned and redox changes in the polymer occur, the probe ion, if it is participating in the doping process, will move in and out of the polymer—the result being that there is either an increase or a decrease in the probe ion concentration reaching the ring. This change in concentration will be reflected as a variation in the otherwise constant ring current, $i_{r,0}$. If $i_r(t)$ is the actual ring current, "the corrected ring current", $i'_r(t)$, can be defined as

$$i'_r(t) = i_r(t) - i_{r,0} \quad (1)$$

Finally, the fraction of the doping change in the polymer due to transport of the probe ion is

$$f_i = -i'_r(t)/(N(i_d(t))) \quad (2)$$

where N, the collection efficiency, is a constant of the particular electrode being used and $i_d(t)$ is the disk current due to polymer redox changes. When all of the doping change is due to the probe ion, $-i'_r(t) = i_d(t)N$ and $f_i = 1$ in eq 2.[25] Finally, if it were possible to measure f_i for each type of ion involved in doping, these would sum up to 1.

The requirements imposed by the RRDE experiment on the redox chemistry of the probe ions limits the selection. For polypyrrole, the same reducible methylpyridinium cations utilized in our earlier studies of pPY^+/pSS^- composites are appropriate.[24] The selection of acceptable probe anions is also narrow. Fortunately, both chloride and bromide meet all of the required criteria.

In the following, we present our results from doping studies on noncomposite, electrochemically grown films of polypyrrole. A collection of different electrolyte ions has been considered. In some instances only the anion or the cation was electrochemically active, but in others both ions were electroactive. *To our knowledge these latter measurements constitute the first successful attempt at quantitatively and independently following the fluxes of both anion and cation dopants in real time during the voltammetry of a single conducting polymer film.*

Experimental Section

Chemicals and Equipment. All chemicals used for this study were purchased from Aldrich. Pyrrole was distilled under nitrogen prior to use and was stored in the dark at 0 °C. Bis(triphenylphosphoranylidene)ammonium tetrakis(3,5-bis(trifluoromethyl)phenyl)borate (PPNBArF) was prepared via metathesis from the chloride and potassium salts of the respective ions. A solution of PPNCl in hot methanol was quickly added to an equimolar amount of potassium tetrakis-(3,5-bis(trifluoromethyl)phenyl)borate (KBArF) also dissolved in hot methanol. Immediately upon mixing, a grainy white solid forms. After the solution cooled, the solid was removed via filtering and recrystallized from *tert*-butyl alcohol. The product was filtered, rinsed with *tert*-butyl alcohol, and dried several hours under vacuum.

Synthesis of KBArF followed a slight modification of a literature procedure for the synthesis of NaBArF. In our procedure, 3,5-bis(trifluoromethyl)benzylmagnesium bromide was reacted with boron trifluoride etherate instead of sodium tetrafluoroborate.[26] The crude product was converted to the potassium salt using potassium carbonate instead of sodium chloride.

(22) Lien, M.; Smyrl, W. H.; Morita, M. *J. Electroanal. Chem.* **1991**, *309*, 333.
(23) Ren, X.; Pickup, P. G. *Electrochim. Acta* **1996**, *41*, 1877.
(24) Salzer, C. A.; Elliott, C. M.; Hendrickson, S. M. *Anal. Chem.* **1999**, *71*, 3677.
(25) This treatment assumes reduction of cations and oxidation of anions (which is the case in the present study). If the opposite redox chemistry occurs (e.g., the probe anion is reduced), the opposite sign of the current applies.
(26) Bahr, S. R.; Boudjouk, P. *J. Org. Chem.* **1992**, *57*, 5545.

PPNBr was prepared by stoichiomeric addition of NaBr to a solution of PPNCl in acetone. After 6 h of stirring, a fine solid (sodium chloride) was present in the flask. The mixture was filtered and the solution collected. The solution was then rotovapped to dryness, leaving a white solid (PPNBr) in the flask. The PPNBr was recrystallized from ethyl acetate/2-propanol. The resulting crystals were dried under vacuum.

1-Methyl-3-cyanopyridinium tetrakis(3,5-bis(trifluoromethyl)phenyl)borate (CMPBArF) was prepared by combining stoichiometric amounts of KBArF and $CMPPF_6$ in hot distilled water. The resulting solid was filtered and rinsed with distilled water. The solid was recrystallized from methanol/water. An analogous process was used for preparation of 1,3-dimethylpyridinium tetrakis(3,5-bis(trifluoromethyl)phenyl)borate (DMPBArF). The synthesis of $CMPPF_6$ and $DMPPF_6$ has been reported previously.[24]

Cells and Electrodes. The electrochemical cells used in film growth and in ring−disk experiments were each single-compartment cells and were employed in a three- or four-electrode configuration, respectively. The platinum ring−disk working electrode employed here has previously been described in detail.[24] A platinum wire was used for the counter electrode, and a Ag/Ag^+ (0.10 M $AgNO_3$, DMSO) reference electrode was employed for film growth. For the ring−disk experiments, a 3 mm diameter Ag disk pseudoreference electrode (−90 ± 50 mV vs SSCE) was utilized. This reference electrode was epoxied into the center of the bottom of the cell to minimize *iR* effects. The instrumental setup has been reported previously.[24]

Film Growth. Films were grown to a variety of thicknesses potentiostatically, galvanostatically, and by potential cycling. Different electrolyte anions were considered (e.g., *p*-toluenesulfonate (Tos^-), hexafluorophosphate (PF_6^-), or tetrafluoroborate (BF_4^-)) as well as different solvents (propylene carbonate and acetonitrile). Very little variation was found in the doping behavior among films produced under each of these conditions. Consequently, polypyrrole films described herein were grown potentiostatically at +0.8 V vs Ag/Ag^+ (0.10 M $AgNO_3$/DMSO) from acetonitrile solutions of pyrrole (0.2 M) and the tetraethylammonium salt (0.2 M) of Tos^-, PF_6^-, or BF_4^-. The extent of film growth was determined by the coulombs passed during polymerization (15 mC, except where noted). Following film growth, the working electrode was removed from the growth solution with the polymer in an oxidized state. The film and electrode were rinsed with copious amounts of acetonitrile and immediately transferred to the RRDE cell.

Cyclic Voltammetry. All voltammetry was performed with rotation of the working electrode at 400 rpm. Unless otherwise stated, a scan rate of 50 mV/s was employed.

Scanning Electron Microscopy (SEM). Scanning electron micrographs were taken using a Phillips model 505 scanning electron microscope. Sample films for imaging were grown onto platinum foil electrodes of approximately identical area. Film thicknesses were monitored with a coulometer and were grown identically as above. The films, in an oxidized state, were dried prior to examination. Gold was sputtered onto the films to a thickness of 20 nm prior to imaging.

Results

General Considerations. The background electrolyte, PPNBArF, was chosen for its electrochemical inactivity and steric bulk. PPN^+ is roughly cylindrical in shape with a van der Waals length of 10.9 Å and a diameter of 8.4 Å. $BArF^-$ is roughly spherical with a diameter of 14.2 Å.[27] In earlier studies with pPY^+/pSS^- composite films, we had found that both PPN^+ and $BArF^-$ were completely excluded from access to the bulk of these composites.[24] We thus assumed that the same result would be obtained with noncomposite polypyrrole films. This proved to be only partially true, as will be discussed subsequently.

(27) Size estimates were made using CAChe Editor, Release 3.9.

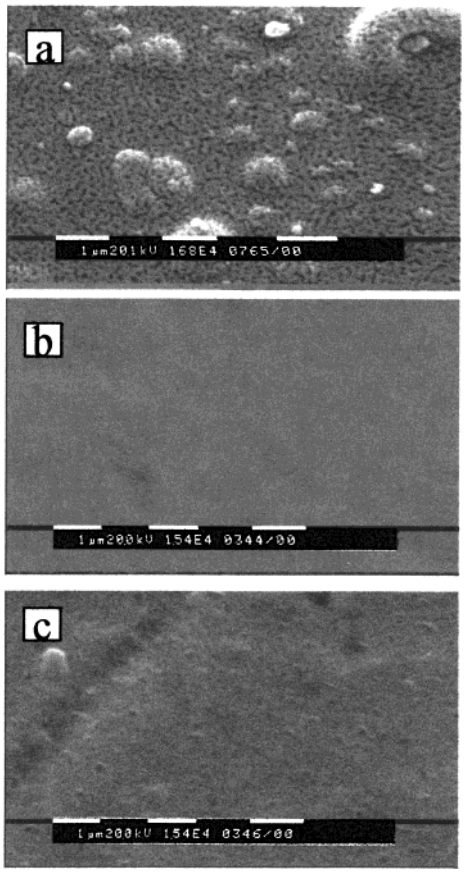

Figure 1. Scanning electron micrographs of (a) pPY/BF_4, (b) pPY/pSS, and (c) $pNMPY/BF_4$.

Various dopant ions were examined in combinations and individually. Individual ion types were introduced into solution as either the PPN^+ or $BArF^-$ salt. The electroactive cations used were 1-methyl-3-cyanopyridinium (CMP^+) and 1,3-dimethylpyridinium (DMP^+); the electroactive anions were Br^- and Cl^-. No difference in interactions with the polymer was found between Cl^- and Br^- or between DMP^+ and CMP^+; the results are thus interchangeable within each pair. Finally, several small electrochemically *inactive* cations and anions (i.e., ions which show no redox activity in the potential window used in this study) were also examined in combination with a redox-active counterion.

Microscopic Film Morphology. SEM. Scanning electron micrographs of three different electrochemically deposited polymers are shown in Figure 1. Figure 1a shows a polypyrrole film. Parts b and c of Figure 1 show a pPY^+/pSS^- composite film[10] and a poly-*N*-methylpyrrole film, respectively. At the resolution of these images, the latter two films are structureless and smooth. In contrast, the polypyrrole film consists of interpenetrating pitted nodules ranging in size down from ca. 1 μm diameter.

Voltammetry of Polypyrrole in PPNBArF Electrolyte. The solid curve (a) in Figure 2 is a voltammogram of a typical polypyrrole film in acetonitrile containing 50 mM PPNBArF. The voltammogram exhibits two obvious pairs of waves: one centered at about −0.25 V and a broader pair centered at 0.10 V. Under identical conditions pPY^+/pSS^- and poly-*N*-methylpyrrole yield

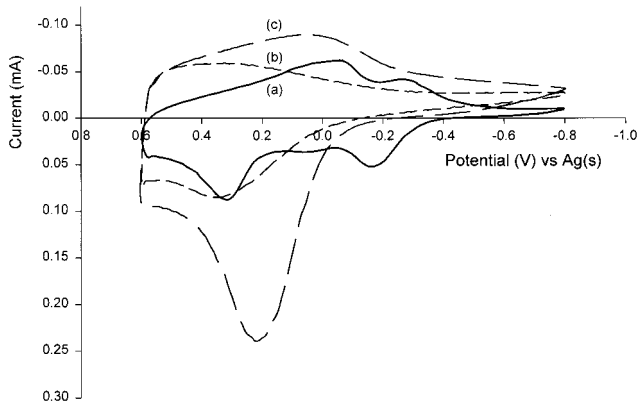

Figure 2. Steady-state cyclic voltammograms of a pPY/PF_6 film at a Pt disk in different combinations of electrolyte. The film is cycled in acetonitrile solutions of 50 mM PPNBArF (a), in 50 mM PPNBArF/2 mM PPNBr (b), and in 50 mM PPNBArF/2 mM PPNBr/2 mM CMPBArF (c).

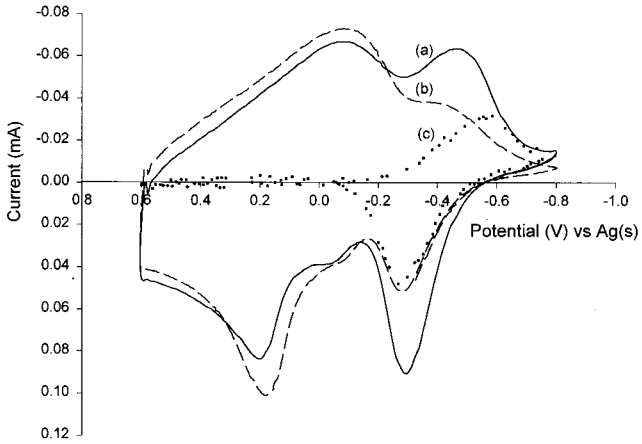

Figure 3. The solid line (a) shows the first cycle of the voltammetry of a pPY/BF_4 film in 50 mM PPNBArF/acetonitrile solution after addition of 2 mM CMPBArF. Prior to the addition of CMPBArF, the film was cycled in 50 mM PPNBArF/acetonitrile until stable voltammetry was obtained. The dashed line (b) is the fifth cycle after addition of CMPBArF, which clearly shows the change in the film voltammetry with continued cycling. The dotted line (c) is a plot of the quantity $-i'_r(t)/N$ for the reduction of CMP^+ correlating with the solid line disk voltammogram (a).

featureless voltammograms with small-magnitude currents characteristic of double-layer charging. In contrast, the charge passed by polypyrrole films in PPNBArF electrolyte is a significant percentage of the total charge capacity of the film, indicating that the PPN^+ and the $BArF^-$ ions are only partially excluded from the bulk of the polymer (vide infra).

Electroactive Cation Doping. CMP^+. Figure 3 shows the polymer voltammetry at the disk (solid curve, a) and the quantity related to the ring current, $-i'_r(t)/N$, for CMP^+ reduction (dotted curve, c) during the first potential scan after CMP^+ is introduced to a solution of 50 mM PPNBArF. The presence of this small cation initially produces only modest changes in the film voltammetry. The major consequence is an immediate increase in the magnitude of the disk current for the process at ca. −0.3 V with very little change in the wave at more positive potentials (cf. Figures 2a and 3a). Note that there is no involvement of CMP^+ in the polymer doping at potentials positive of 0.0 V. From the ring current data in Figure 3, it is evident that the entire increase in current at the disk can be attributed to CMP^+ doping in the polymer. With continued potential cycling, the wave at −0.3 V diminishes and finally disappears after ca. 10 cycles. Concomitantly, the changes in ring current reflected by the quantity $-i'_r(t)/N$ shows that doping by CMP^+ diminishes as well, eventually reaching zero. Finally, as the wave at −0.3 V decreases, both the oxidation and reduction currents at more positive potentials increase (Figure 3b).

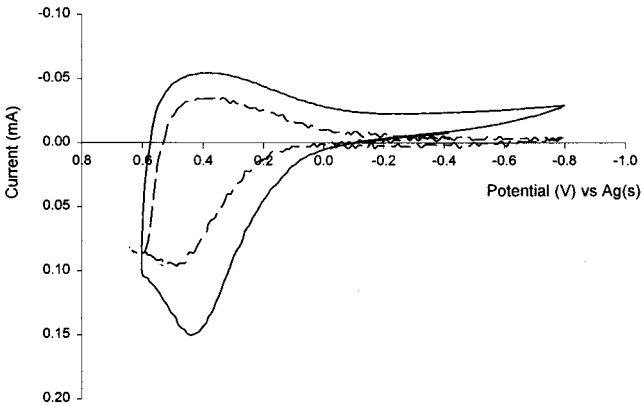

Figure 4. The solid line shows the current response for a pPY/PF_6 film cycled in an acetonitrile solution of 50 mM PPNBArF/2 mM PPNCl. The oxidation of Cl^- at the ring electrode (presented as $-i'_r(t)/N$) is given by the dashed line.

Electroactive Anions. Cl^- or Br^-. Contrasted with the minor changes in the polypyrrole voltammetry brought about by the addition of CMP^+, introduction of PPNBr or PPNCl causes profound changes that are evident by comparison of curves a and b in Figure 2. The voltammogram of the film becomes rather featureless with a broad oxidation peak at ca. 0.4 V. The wave on the reduction scan is also very broad, extending past the negative potential limit back into the anodic sweep. This type of behavior, as will be discussed in more detail subsequently, is indicative of slow ion transport within the polymer. A typical measurement of $-i'_r(t)/N$ for the doping by a halide is shown in Figure 4. Although the ring voltammetry shows a significant amount of charge compensation by the halide, there is obviously additional doping by electrochemically inactive ion(s); otherwise, the magnitude of $-i'_r(t)/N$ and disk current (dashed and solid curves in Figure 4, respectively) would be identical.

Electroactive Cation and Anion. CMP^+ and Cl^-. Figure 2c demonstrates the effect on the polypyrrole voltammetry of adding CMP^+ into a solution already containing Cl^-. When the CMP^+ is added, the total charge capacity of the film within the voltage range scanned approximately doubles and a relatively sharp peak at ca. 0.2 V develops on the anodic scan. Additionally, the cathodic current at negative potential increases.

Figure 5 shows $-i'_r(t)/N$ for CMP^+ reduction (Figure 5b) and of Cl^- oxidation (Figure 5c) for a typical polypyrrole film that has been potential-cycled to steady state in acetonitrile solution containing 2 mM CMPCl and 50 mM PPNBArF. Negative of ca. 0.0 V the doping change is predominantly due to CMP^+. In fact, except at the positive extreme of the potential scan, the doping change shows a considerable contribution from CMP^+.

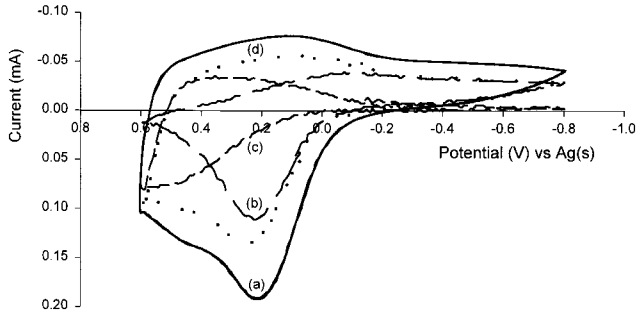

Figure 5. The current response of a pPY/PF_6 film cycled in an acetonitrile solution of 50 mM PPNBArF/2 mM CMPBArF/2 mM PPNCl is shown by the solid line voltammogram (a). The current response, $-i'_r(t)/N$, for CMP^+ reduction and for Cl^- oxidation at the ring are given by the long dashed line (b) and short dashed line (c) voltammograms, respectively. The dotted line voltammogram (d) shows the sum of the CMP^+ and Cl^- contributions to the film doping. Note the relationship of the shape and magnitude of this voltammogram (d) with the total film voltammetry (a). The voltammogram of the film (a) and the total electroactive ion voltammogram (d) do not exactly overlay as a result of partial doping by PPNBArF.

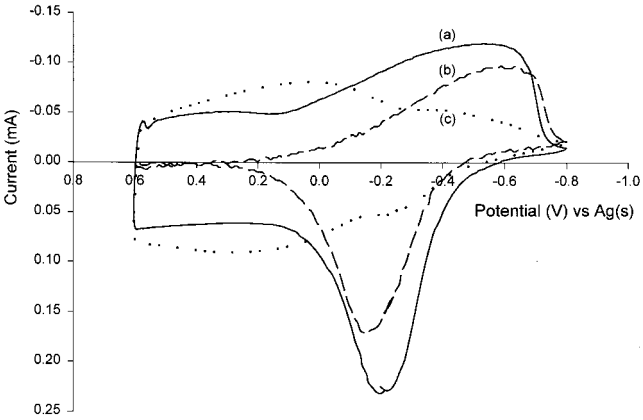

Figure 6. The voltammetric response of a pPY/Tos film cycled in an acetonitrile solution of 50 mM PPNBArF/2 mM $PPNPF_6$ is given by the solid line (a). The ring current response, $-i'_r(t)/N$, for the reduction of CMP^+ for the first cycle after addition of CMPBArF (2 mM) is plotted by the dashed line (b). The dotted line (c) is the disk current response after ca. 10 cycles.

Chloride doping only becomes significant at the most positive potentials ($E > 0.4$ V).

Electrochemically Inactive Cations. TAA^+ (Tetraalkylammonium). Various electrochemically inactive cations (tetrabutyl-, tetrapropyl-, and tetramethylammonium) were added to background electrolyte solutions as Cl^- salts. The resulting film voltammetry depends on which cation is present. Adding TBACl or TPrACl produces voltammetry similar to that obtained in PPNCl electrolyte (cf. Figure 2b). Adding TMACl, on the other hand, results in voltammetry at both the disk and ring (for Cl^- oxidation) similar to that obtained from CMPCl (cf. parts a and c of Figure 5), indicating that TMA^+ participates in the doping much like CMP^+.

Electrochemically Inactive Lipophilic Anion. PF_6^-. Addition of $CMPPF_6$ to the background electrolyte solution results in polymer voltammetry qualitatively similar to that in CMPBArF (cf. Figures 3 and 6) except that more CMP^+ doping is evident. The pair of peaks at ca. −0.3 V (Figure 6) initially grows in magnitude, but then decreases with time until it is no longer observable. The evolution of the CMP^+ voltammetry tracks the growth and disappearance of this peak just as it did for CMPBArF.

Discussion

Considering the scanning electron micrographs of the three polymer films shown in Figure 1, only polypyrrole has resolvable structure at these magnifications. Also, polypyrrole is the only one of these three polymers that exhibits any significant redox activity in PPNBArF electrolyte. Typically, the total integrated charge passed by a polypyrrole film cycled over the potential region between +0.6 and −0.8 V vs Ag/Ag^+ is about 60% as large in PPNBArF electrolyte as in $TMAPF_6$. The increased charge capacity with $TMAPF_6$ shows that there are some polymer redox sites (roughly 40%) accessible only to smaller ions. The linear relationship between the scan rate and the peak currents of the polymer voltammetry in PPNBArF electrolyte, however, indicates that ion transport within the polymer is rapid, at least for scan rates in the range of 25−100 mV/s.

From the CV data and the SEM images we can now make some reasonable inferences about the nanoscopic structure of these polypyrrole films. For there to be rapid transport of PPN^+ and $BArF^-$ within the polymer, channels must exist which are several times the diameter of the ions; otherwise, we would expect slow ion transport, which would show up in the scan rate dependence of the polymer CV. Furthermore, slightly more than half of the total redox centers must be close enough to the walls of these channels to be charge compensated by ions in the channels. The remaining sites are not so close, but some fraction of these (maybe all) can be rapidly accessed by smaller TMA^+ and PF_6^- ions. This model is consistent with the SEM image (Figure 1a) that shows a porous structure that, on the basis of the CV results, must extend down to the dimension of tens of angstroms. Likewise, the featureless SEM images of pPY^+/pSS^- and poly-*N*-methylpyrrole are consistent with their lack of electrochemistry in PPNBArF electrolytes.

The initial increase in polymer current resulting from the addition of CMPBArF quantitatively tracks the polymer incorporation of CMP^+ (cf. Figure 3). For CMP^+ (or any cation) to participate in doping requires the presence of "fixed" anionic sites within the polymer. Since the charge on the polypyrrole backbone is either neutral (when fully reduced) or positive (when oxidized), these negatively charged sites must result from anions that were entrapped during the growth process. Thus, when the polypyrrole is reduced, cations from solution incorporate to balance the negative charge of the entrapped anion. For reasons that are not transparent, these sites are the most difficult ones to be reduced and easiest to be oxidized (i.e., they have the most negative redox potential). The similarity in the general shape of the polymer voltammograms in Figures 2a and 3a suggest that a significant number of these trapped anion sites are close to the surface of the nanoscopic pores and can thus be compensated by PPN^+. Interestingly, the very process of repeated doping and undoping with CMP^+ (or other small cations) modifies the polymer structure in a way that releases the entrapped anions. Once this is accomplished, no further CMP^+ doping is evident from the ring current. In contrast, cycling the

polymer in PPNBArF alone gives steady-state voltammetry of the types observed in Figure 2a where there is an obvious stable cation-doping peak at −0.3 V. Also, addition of tetramethylammonium ion (TMA^+) to solution causes changes in the polymer voltammetry very similar to those observed with addition of CMP^+. This suggests that the behavior of CMP^+ is not unique, but rather, it is a general "small cation" effect. In contrast to TMA^+, the addition of modestly larger cations, such as tetrapropylammonium, produces no changes in the polymer voltammetry, thus indicating that it is excluded from sites accessible to CMP^+ and TMA^+ (ostensibly, because of size).

As described previously, when CMP^+ is introduced with a small, lipophilic anion such as BF_4^-, PF_6^-, or Tos^- rather than as the $BArF^-$ salt, the interaction between CMP^+ and the polymer is qualitatively similar to that observed for the case of CMPBArF. The only difference is that the amount of CMP^+ doping is initially larger. Essentially the same steady-state voltammetry results from each of these anions; namely, the current−potential profile is broadened and the charge capacity, especially at more positive potentials, is increased. This increased charge capacity must reflect the greater number of redox sites accessible to the smaller anions. Therefore, we conclude that, at steady state, some combination of small anion and $BArF^-$ is responsible for *all* charge compensation changes of the polymer (i.e., no cation participation).

The addition to solution of PPNX, where X^- is Br^- or Cl^-, produces dramatically different changes in the polymer voltammetry relative to, for instance, $PPNPF_6$. On the first anodic cycle after PPNX is introduced to the solution, 30% more charge is passed during the polymer oxidation than passes on the subsequent re-reduction cycle. After the first exposure to X^- at positive potentials, visible examination of the film color indicates that the polymer never fully reduces again. In other words, roughly one-third of the X^- that enters the film on the first oxidation cycle does not come back out. Also, as is evident from Figure 4, no significant amount of X^- (in this specific case, Cl^-) participates in doping changes negative of ca. −0.1 V despite considerable current being passed at the disk.

As pointed out in the Results, addition of CMP^+ (or other small organic cations, e.g., TMA^+) to a solution already containing X^- results in a roughly 2-fold increase in the total charge capacity of the film (cf. Figure 2). Interestingly, adding CMP^+ causes virtually no change in the shape or magnitude of the doping profile of X^-; all of the additional charge capacity can be attributed to CMP^+ doping (cf. Figures 2 and 5). Figure 5 is typical of the steady-state voltammetry obtained with CMP^+ and X^- present in solution. Both ions contribute to the doping change, which is in contrast to the behavior of CMP^+ in the presence of PF_6^-, BF_4^-, or Tos^-, where there is no cation participation at steady state.

Earlier, the linear relation of the scan rate and the peak currents of the polypyrrole voltammetry was invoked to argue that, in the absence of X^-, ion transport within the film is facile. Ions of both charges appear to move rapidly within whatever polymer domain(s) is accessible to them (determined by their size). The initial irreversible uptake of X^- eliminates this rapid ion transport within the polymer. This is demonstrated by the fact that on the positive-going scan potentials up to ca. −0.2 V *cathodic* current continues to flow (Figure 4, solid line). Such behavior is consistent with the redox process having become mass-transport-limited; that is, the film is not equilibrated to the redox potential due to the slow incorporation or transport of the counterions. Since the quantity $-i'_r(t)/N$, shown in Figures 4 and 5 for halide oxidation, gives no indication that X^- is participating in doping changes in this potential range, presumably charge balance is being maintained by cation uptake. The ring voltammetry in Figure 5 corroborates this assertion as evidenced by the contribution of CMP^+ in this potential region. It would appear that the initial irreversible uptake of Cl^- dramatically alters the structure of the polymer in a way that profoundly affects ion (and presumably solvent) transport into and/or through the polymer.

Another unusual feature of the polymer voltammetry in CMPX electrolyte is the existence of significant potential regions, during both the anodic and cathodic scans, where both CMP^+ and X^- are simultaneously participating in the doping change. For example, from approximately 0.2 to 0.6 V on the anodic scan in Figure 5 significant uptake of Cl^- and loss of CMP^+ are simultaneously occurring. Clearly a simple Donnon exclusion model is incapable of explaining such complex behavior.

From all of the various RRDE data collected here, we can begin to construct a model that can explain the redox behavior of polypyrrole in contact with X^- electrolyte. Before doing so, it is useful to recount briefly the major findings of our earlier RRDE study of pPY^+/pSS^- films. Succinctly put, all doping changes in these composite films are *quantitatively* due to small-cation (e.g., CMP^+) transport. When the films are first grown electrochemically, pSS^- polyanions are irreversibly incorporated. Subsequently, when the polypyrrole backbone is reduced, the influx of small cations into the polymer is the only mechanism available to maintain charge neutrality.

The doping behavior of polypyrrole in PPNX or CMPX electrolytes is probably best characterized (phenomenologically, at least) as being hybrid between the doping behavior of pPY^+/pSS^- composites and that of the other small-ion systems considered here (e.g., $CMPPF_6$). The fraction of X^- that irreversibly enters the film on the first anodic scan behaves similarly to pSS^-; i.e., they serve as permanent negative charges that do not leave the polymer on the time scale of the experiment. To reduce those cationic sites on the polypyrrole that are associated with these "fixed" X^- sites requires that some other cation enter the film to balance the charge. The remaining "mobile" X^- can move out of the polymer to maintain charge neutrality. If the only cation in solution is PPN^+, only a relatively small quantity of these ions can enter the now-more-restricted pore structure of the polymer on the time scale of the experiment. The mobile X^- ions, on the other hand, can come and go as redox changes of the polymer require; thus, they dominate the doping change when PPN^+ is the only cation available. When a small cation such as CMP^+ is introduced into solution, it can more easily and quickly enter the

polymer. Thus, all of the sites compensated by mobile X^- can still undergo reduction, but additionally, a significant fraction of polypyrrole sites compensated by fixed X^- can now also reduce because CMP^+ can enter the polymer to replace the oxidized cationic polypyrrole sites. Interestingly, the sites associated with the fixed X^- are the easiest to oxidize and hardest to reduce. In other words, starting at the most reducing potentials, it is thermodynamically easier to expel CMP^+ than to incorporate additional X^-.

Finally, the uptake of X^- by the polymer is only "irreversible" to the extent that the film remains in contact with X^--containing electrolyte. Transferring the film back into a solution of PPNBArF restores the original shape of the voltammogram (i.e., as in Figure 2 or 3). The polymer also regains the capability of being fully reduced at negative potentials after several potential cycles in the new electrolyte.

Conclusion

We have shown that RRDE voltammetry is a useful tool in quantitatively mapping the complex changes in the ionic composition of polypyrrole films under conditions of electrochemical control. By considering electrolyte solutions containing various combinations of electrochemically active probe ions and electroinactive ions, a wide range of solution electrolyte conditions can be investigated. Contrary to preconceived expectations, the method by which the polypyrrole films are grown (i.e., potentiostatically, galvanostatically, or via potential cycling) has practically no effect on the doping behavior. Instead, the doping behavior is entirely dominated by the nature and combination of ions available to the films from the electrolyte solution. In the presence of small organic cations and lypophilic anions, for example, anion transport dominates doping changes at steady state (which is the same behavior typically reported by others who have studied similar films by indirect methods). However, prior to reaching steady state both ion types are involved.[3,4,7] In contrast, electrolytes containing small, hard anions (i.e., Br^- and Cl^-) drastically (but reversibly) alter the doping profile of polypyrrole and probably alter its nanoscopic structure. These anions enter the polymer and, in part, become entrapped such that cation doping is required to discharge (reduce) the polypyrrole sites with which the entrapped anions are associated. Finally, electrochemically grown films of polypyrrole have a porous structure that is clearly evident from SEM images; moreover, that porosity extends down to the dimensions of the electrolyte ions. Otherwise, large electrolyte ions such as PPN^+ and $BArF^-$ would be sterically excluded from the bulk of the polymer, as they are by pPY^+/pSS^- and poly-*N*-methylpyrrole.[24]

Acknowledgment. We acknowledge support of this work by the National Science Foundation (Grant CHE-971408). We also thank Shawn Sapp for his assistance in obtaining the SEM images.

CM0000189